


 Cite this: *CrystEngComm*, 2017, 19, 6067

Recent progress in the synthesis of nanostructured magnesium hydroxide

 Giulia Balducci, Laura Bravo Diaz  and Duncan H. Gregory *

This review highlights synthetic routes for producing nanostructured magnesium hydroxide and focuses on how these various preparative approaches can produce $\text{Mg}(\text{OH})_2$ nanoparticles with controlled size and morphology. $\text{Mg}(\text{OH})_2$ nanocrystals with rod-, needle-, hollow tube- or platelet-like morphology can be synthesised by the modification of chemical and physical experimental parameters such as the selection of magnesium precursor, solvent and temperature or by employing surface modifiers and templates. Techniques based on hydrothermal/solvothermal treatments, microwave heating and (co-)precipitation are dominant in the production of $\text{Mg}(\text{OH})_2$ at the nanoscale, but other materials design approaches are now emerging. Bulk $\text{Mg}(\text{OH})_2$ has been extensively studied over decades and finds use in a wide range of applications. Moreover, the hydroxide can also serve as a precursor for other commercially important materials such as MgO . Nanostructuring the material has proven extremely useful in modifying some of its most important properties – not least enhancing the performance of $\text{Mg}(\text{OH})_2$ as a non-toxic flame retardant – but equally it is creating new avenues of applied research. We evaluate herein the latest efforts to design novel synthesis routes to nano- $\text{Mg}(\text{OH})_2$, to understand the mechanisms of crystallite growth and to tailor microstructure towards specific properties and applications.

 Received 30th August 2017,
Accepted 3rd October 2017

DOI: 10.1039/c7ce01570d

rsc.li/crystengcomm

Introduction

Magnesium hydroxide (MH), $\text{Mg}(\text{OH})_2$, naturally occurring as the mineral brucite, has attracted much attention over the past decades. $\text{Mg}(\text{OH})_2$ is a white, odourless solid

WestCHEM, School of Chemistry, University of Glasgow, Glasgow G12 8QQ, UK.
E-mail: Duncan.Gregory@Glasgow.ac.uk



Giulia Balducci

energy storage materials, with particular emphasis on nanostructured hydrogen and ammonia storage solutions.

Dr Giulia Balducci graduated from the University of Bologna with an MSc degree in chemistry in 2009. Following the award of two consecutive research bursaries to perform research at the University of Bologna, she moved to the University of Glasgow, where she graduated with a PhD in 2015 under the supervision of Professor Duncan H. Gregory. She worked as a postdoctoral researcher at Glasgow until April 2016. Her research focuses on



Laura Bravo Diaz

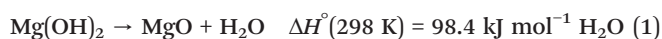
2013 she has undertaken PhD studies in Chemistry at the University of Glasgow under the supervision of Professor Duncan H. Gregory while based also at the DG JRC as a research fellow in hydrogen storage technologies. Her research interests include the synthesis and characterisation of advanced nanomaterials and their applications in energy conversion and storage.

Laura Bravo Diaz received an MEng degree in chemical engineering from the University of Cantabria, Spain, in 2010. From 2010–2012 she worked as a junior engineer in the renewable energy research sector before joining the European Commission DG Joint Research Centre (DG JRC) as an early-stage-researcher at SolTeF, the EU reference laboratory on hydrogen storage capacity measurements in solid-state materials. Since



characterised by an extremely low solubility in water (0.009 g L⁻¹ at 18 °C) and a refractive index $n_D = 1.559$.¹ MH crystallises in the tetragonal $P\bar{3}m1$ space group, with lattice parameters of $a = 3.148 \text{ \AA}$ and $c = 4.779 \text{ \AA}$ (Fig. 1).^{2,3} In the $\text{Mg}(\text{OH})_2$ crystal structure, each magnesium, Mg^{2+} , cation is coordinated by 6 hydroxide, OH^- anions to form $\text{Mg}(\text{OH})_6$ octahedra, which share faces in two dimensions resulting in a layered structure. Conversely, each OH^- anion is surrounded by three Mg^{2+} cations in a pyramidal geometry. The oxygen atoms in the OH^- anions are located in planes above and below the planes of Mg^{2+} cations with O–H bonds perpendicular to these metal-containing planes. The extended crystal structure is completed in the third dimension by hydrogen bonding, which weakly binds the hexagonal close packed (HCP) anion layers together, with a shortest $\text{H}\cdots\text{H}$ interlayer distance of 1.97 Å. The $\cdots\text{ABABA}\cdots$ HCP layers are spatially distributed such that the hydroxide hydrogens within one layer point towards the centre of the triangular plane (an $\text{Mg}(\text{OH})_6$ octahedral face) formed by 3 OH bonds in the next layer.

When heated to temperatures above 350 °C, bulk $\text{Mg}(\text{OH})_2$ undergoes a dehydration process resulting in the formation of MgO (cubic, $Fm\bar{3}m$)⁵ and the evolution of water (eqn (1)).^{6,7}



The ability of the hydroxide to decompose endothermically releasing water and forming MgO without the production of corrosive or toxic by-products, accounts for its major importance as a commercial non-toxic flame retardant. Magnesium hydroxide also finds application as an acidic waste neutraliser, as a pharmaceutical excipient, in paper conservation, as a component in ethanol chemical sensors and as the most important precursor for the preparation of (nanostructured) magnesium oxide which, in turn, finds application in catalysis.^{6,8–16}



Duncan H. Gregory

and properties of sustainable energy materials, functional materials and nanomaterials.

Duncan H. Gregory studied at the University of Southampton completing a PhD in solid state chemistry in 1993 under Prof. Mark Weller. He was an EPSRC advanced fellow, lecturer and reader in materials chemistry at the University of Nottingham until 2006. He then took the WestCHEM chair in inorganic materials in the School of Chemistry at the University of Glasgow. His research interests centre on the synthesis, structure

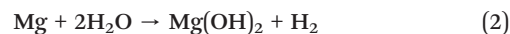
A variety of methods for yielding nanostructured $\text{Mg}(\text{OH})_2$ have been reported. These include hydrothermal/solvothermal techniques, precipitation routes and microwave-assisted methods. Further, the use of surfactants and templating agents has been explored as a means to obtain $\text{Mg}(\text{OH})_2$ nanocrystals with different morphologies, from hexagonal nanoplates through nanotubes, nanorods and nanosheets to mixture of nanosheets and nanoparticles. However, due to the fact that surfactants are not environmentally sustainable and that their employment results in an additional cost to processing, efforts have been made in order to remove them from the synthetic procedure. Similar environmental concerns arise for synthetic procedures involving non-aqueous solvents, which are commonly used in solvothermal reactions. Ultimately, the goal for the production of $\text{Mg}(\text{OH})_2$ is to find novel synthetic routes that are fast, simple, energy-efficient and allow fine control over particle size and morphology. Below we discuss and highlight the latest progress made in terms of synthetic routes to yield nanostructured magnesium hydroxide.

Synthetic routes to nanostructured $\text{Mg}(\text{OH})_2$

Conventional hydrothermal/solvothermal synthesis

Hydrothermal and solvothermal methods have been widely employed to produce nanostructured $\text{Mg}(\text{OH})_2$. These methods often involve the use of surfactants such as poly(ethylene glycol) (PEG) or ethylenediamine (en), which are considered to play an important role in the mechanism of the nanostructure formation, acting either as templates or growth inhibitors. One of the major drawbacks of these synthetic procedures however is the relatively long reaction time, which is typically of 6 to 24 h or more. Nonetheless, hydro/solvothermal treatments have been extensively explored in terms of morphology and size control for the synthesis of nano-MH.

The synthesis of $\text{Mg}(\text{OH})_2$ nanorods by solvothermal treatment was first reported in 2000 by Li *et al.*¹⁷ In the experimental procedure Mg metal was used as magnesium source and en as a templating agent. The hydrothermal reaction (eqn (2)) leads to the production of rod-like nanoparticles in a process described as “soft templating”.



The key influence in the crystal growth mechanism is believed to be the presence of the en molecules, which are likely to act as bidentate ligands to form a complex with Mg^{2+} cations, thereafter controlling the nucleation and growth of the nanorods. The stability of such a complex is expected to decrease as temperature and pressure are increased, coordinating the OH^- groups present in solution to the complex and causing the 1D nanorod structures to condense. Ultimately, the Mg–N bonds to the donor ligands



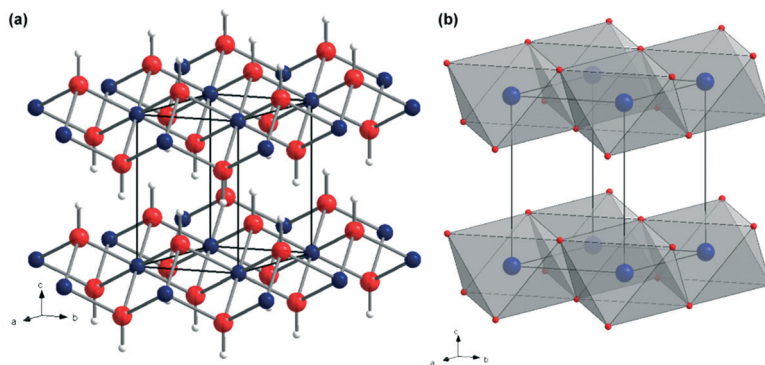


Fig. 1 Crystal structure of $\text{Mg}(\text{OH})_2$: (a) as a ball-and-stick representation with Mg as blue spheres, O as red spheres and H as white spheres, respectively; (b) as a polyhedral representation showing layers of face-sharing $\text{Mg}(\text{OH})_6$ octahedra connected along the $\langle 001 \rangle$ direction via hydrogen bonding (adapted from ref. 4).

become weaker whilst Mg–O bonds form gradually until the point is reached where Mg and N are separated from each other and Mg cations are connected to OH^- anions, forming $\text{Mg}(\text{OH})_2$. However, in 2001, Ding *et al.* published a seminal paper in terms of a directed hydrothermal synthesis of $\text{Mg}(\text{OH})_2$. They reported the preparation of nanostructured MH in which one could control size and morphology selectively. Rod-, tube-, needle- or lamellar-like nanoparticles could be produced by varying the aqueous solvent composition as well as the magnesium source (Mg, MgSO_4 and $\text{Mg}(\text{NO}_3)_2$) and tuning the hydrothermal reaction conditions.¹⁸ Ethylenediamine solution, aqueous ammonia or dilute sodium hydroxide solution were investigated as possible solvents and the results obtained are summarised in Table 1.

Two years after Ding *et al.*'s paper, Fan *et al.* reported the development of the above concept by employing en itself as a suitable solvent.¹⁹ The synthesis used nanowires of $\text{Mg}_{10}(\text{OH})_{18}\text{Cl}_2 \cdot 5\text{H}_2\text{O}$ as a magnesium source to yield hollow $\text{Mg}(\text{OH})_2$ nanotubes. The synthesis of the hydrated hydroxide chloride precursor was previously reported by Christensen *et al.*²⁰

Following a synthetic procedure analogous to the one reported by Ding *et al.* (discussed above),¹⁸ it was possible to produce nanotubes defined by outer diameters of 80–150 nm, wall thicknesses of 30–50 nm and lengths of up to 5–10 μm . A growth mechanism has been proposed that involves the exchange of Cl^- and OH^- anions during solvothermal

treatment. The mechanism of crystal growth is consistent with the one originally proposed by Li *et al.*,¹⁷ in which en is also believed to play a pivotal role in controlling the product morphology by acting as a bidentate ligand leading to the production of the one dimensional structure. However, the fibre-like morphology of the magnesium precursor is also believed to be very important, as one might anticipate.¹⁹ In the following year (2004), many of the same researchers published further work providing additional insight into the above-mentioned system together with the study of two other possible solvents: 1,6-diaminohexane and pyridine.²¹ It was found that size and morphology of the hydroxide product were greatly influenced by the solvent used and by the reaction temperature during the solvothermal process. In particular, both en and diaminohexane lead to the formation of nanotubes with outer diameters of 80–300 nm, wall thicknesses of 30–80 nm and lengths of several microns, whilst the use of pyridine resulted in a rod-like morphology. This difference in morphology is attributed to the coordination behaviour of the respective ligands; both en and diaminohexane act as bidentate ligands whereas pyridine is a monodentate ligand. Nonetheless, the mechanism of crystal growth for all structures is believed to be the fundamentally identical to that reported previously (in 2003).¹⁹ Interestingly several years later, high aspect ratio nanowires of “ $\text{Mg}_x(\text{OH})_y\text{Cl}_z \cdot n\text{H}_2\text{O}$ ” were used in the templated pseudomorphic synthesis of MH nanowires (by reaction with NaOH in

Table 1 Nanostructured $\text{Mg}(\text{OH})_2$ obtained under different experimental conditions. Adapted with permission from Y. Ding, G. Zhang, H. Wu, B. Hai, L. Wang and Y. Qian, *Chem. Mater.*, 2001, **13**, 435–440. Copyright 2001 American chemical Society¹⁸

Mg source	Solvent	Temperature (T)/K	Time/h	Morphology	Dimensions/nm
Mg	en– H_2O (8 : 1)	453	20	Rod-like	Diameter: 20, length: 200
Mg	en– H_2O (1 : 6)	453	20	Lamellar	Diameter: 50–100, thickness: 10
Mg	$\text{NH}_3 \cdot \text{H}_2\text{O}$ (pH 10)	453	20	Lamellar; tube-like	Diameter: 25–200; outer diameter: 40, length: 60
MgSO_4	en– H_2O (4 : 1)	453	20	Needle-like	Diameter: 10–20, length: 50–100
MgSO_4	en– H_2O (1 : 1)	453	20	Lamellar	Diameter: 100–150
MgSO_4	$\text{NH}_3 \cdot \text{H}_2\text{O}$ (pH 11)	453	20	Lamellar	Diameter: 150
$\text{Mg}(\text{NO}_3)_2 \cdot 6\text{H}_2\text{O}$	en	453	20	Lamellar	Diameter: 80–100
$\text{Mg}(\text{NO}_3)_2 \cdot 6\text{H}_2\text{O}$	$\text{NH}_3 \cdot \text{H}_2\text{O}$ (pH 10)	453	20	Lamellar	Diameter: 100–200
$\text{Mg}(\text{NO}_3)_2 \cdot 6\text{H}_2\text{O}$	NaOH (0.1 M)	353	2	Lamellar	Diameter: 50



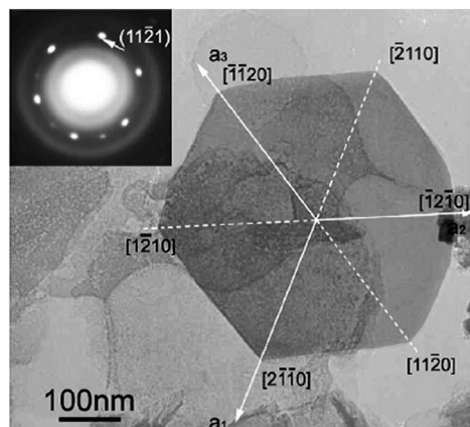


Fig. 4 TEM image and selected area electron diffraction (SAED) pattern (inset) of a regular hexagonal $\text{Mg}(\text{OH})_2$ nanoflake synthesised from $\text{Mg}(\text{NO}_3)_2$ and $\text{N}_2\text{H}_4 \cdot \text{H}_2\text{O}$. Reprinted from *Materials Chemistry and Physics*, **112**, D. Jin, X. Gu, X. Yu, G. Ding, H. Zhu and K. Yao, Hydrothermal synthesis and characterization of hexagonal $\text{Mg}(\text{OH})_2$ nano-flake as a flame retardant, 962–965, copyright 2008, with permission of Elsevier.³¹

lamellar structure, although it is not clear why this should be the case.

More recently, well-dispersed, discrete hexagonal MH nanoflakes were obtained hydrothermally using magnesium nitrate hexahydrate in the presence of the polymeric templating agent, PEG 20000.³² As shown in Fig. 5, the synthesised magnesium hydroxide nanoparticles present a hexagonal flake-like morphology with a thickness of only *ca.* 10 nm, a lateral size of *ca.* 100 nm and a specific surface area of $\sim 69 \text{ m}^2 \text{ g}^{-1}$. In the absence of PEG 20000, similarly prepared MH particles exhibited a higher polydispersity and a slightly reduced specific surface area ($\sim 42 \text{ m}^2 \text{ g}^{-1}$). There is no firm evidence to indicate the exact role played by PEG in the MH nanoflake formation mechanism and the authors speculate that its main functions are to prevent the agglomeration of the hexagonal $\text{Mg}(\text{OH})_2$ nanoflakes and to control the growth rate. The morphology of the synthesised nanocrystals is proposed to originate from the formation of “PEG– Mg^{2+} pairs”. The authors proposed that the “PEG– Mg^{2+} pairs” develop initially *via* complex formation, with PEG coordinat-

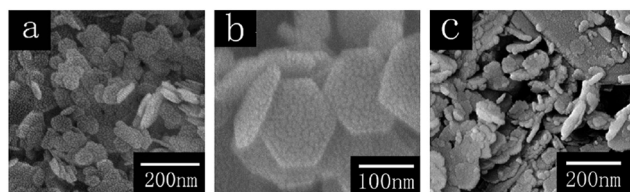


Fig. 5 SEM images of $\text{Mg}(\text{OH})_2$ nanoflakes (a) synthesised with PEG20000 (at low magnification); (b) synthesised with PEG20000 (at higher magnification) and (c) synthesised without PEG 20000. Reprinted from *Materials Research Bulletin*, **51**, Q. Wang, C. Li, M. Guo, L. Sun and C. Hu, Hydrothermal synthesis of hexagonal magnesium hydroxide nanoflakes, 35–39, copyright 2014, with permission of Elsevier.³²

ing to Mg^{2+} ions in $\text{Mg}(\text{NO}_3)_2$ through oxygen donors prior to the hydrothermal treatment. These “PEG– Mg^{2+} pairs” are then proposed to combine during stirring and aging to form a skeleton of PEG chains that are twisted and coiled with each other to form a series of continuous hexagonal pores. When NaOH was added to the system, the OH^- ions are proposed to react preferentially with Mg^{2+} ions located in the hexagonal holes of the entangled PEG skeleton to form small crystal nuclei of magnesium hydroxide. With increasing temperature and time over the period of the hydrothermal treatment, these $\text{Mg}(\text{OH})_2$ crystal nuclei grow until finally they detach from the hexagonal pores (which act as a template). Compared to synthesis and hydroxide growth without PEG, the initial coordination process and the subsequent PEG templating process is predicted to be slow in kinetic terms. It is evident that further syntheses using varying molecular weight polymeric additives and closer scrutiny of the ensuing crystallisation processes are required in order to understand the templated MH growth in such systems more fully and a fuller comparison with PEG-templated coprecipitation methods performed at ambient pressure (see below) would be useful.

From all the examples in this section, it can be seen that hydrothermal/solvothermal methods can be widely utilised to obtain $\text{Mg}(\text{OH})_2$ nanostructures with degrees of control over size and morphology.

The main advantages lie with a high level of reproducibility and generally the method encourages production of 2D plate-like nanostructures with dimensions and porosity that can be modified by appropriate selection of experimental parameters (such as temperature, time and pH) and choice of reagents. Such syntheses typically lead to a low degree of agglomeration and opportunities to produce monodisperse MH particles of high surface area. By contrast, the growth of 1D nanostructures is rarer and more difficult, requiring more “forcing” growth conditions such as the use of hard templates (*e.g.* nanowire precursors). Nevertheless, solvothermal methods allow one to tailor the crystal growth to different morphologies for different applications.

Given the range of chemical variables applied in solvothermal syntheses – such as solvent, magnesium source, molecular (ligating) templating agents (*e.g.* en, en– H_2O , diamino-hexane, pyridine or hydrazine hydrate) or other soft/hard templates – it is difficult to appreciate the precise role of each of these variables in a single set of experiments and even more complex to consider their combinations across multiple synthesis regimes. The nucleation and crystal growth is often initiated by the ability of molecular additives (acting as ligands) to form coordination complexes with Mg^{2+} cations (typically present in a salt precursor or oxidised from Mg metal). To some extent the nanorod, nanoneedle, nanotube or various lamellar morphologies should depend on the coordination behaviour of the respective ligands to the metal centre as well as on the magnesium precursor employed and the morphology of the precursor itself. Syntheses involving aqueous ammonia (for example, in the formation of MH



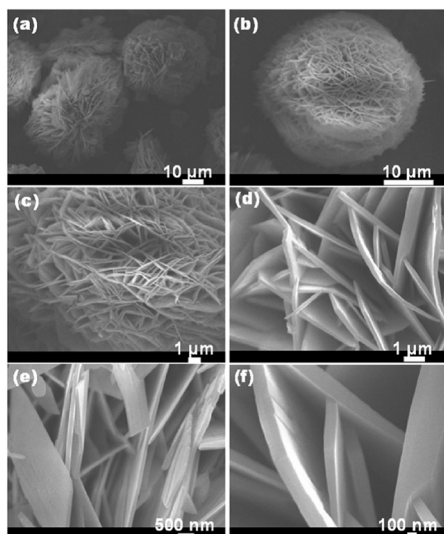
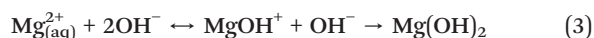


Fig. 6 Typical (a and b) low-magnification and high-resolution (c–f) FESEM images of $\text{Mg}(\text{OH})_2$ nanosheet networks as synthesised via microwave hydrothermal processing. Reprinted from *Journal of Alloys and Compounds*, 519, F. Al-Hazmi, A. Umar, G. N. Dar, A. A. Al-Ghamdi, S. A. Al-Sayari, A. Al-Hajry, S. H. Kim, R. M. Al-Tuwirqi, F. Alnowaiserb and F. El-Tantawy, Microwave assisted rapid growth of $\text{Mg}(\text{OH})_2$ nanosheet networks for ethanol chemical sensor application, 4–8, copyright 2012, with permission of Elsevier.¹³

combination of Mg^{2+} cations with hydroxide ions as follows (eqn (3)):



The MgOH^+ ions (magnesium hydroxo ions) are believed to act as the precursor in producing the $\text{Mg}(\text{OH})_2$ nuclei that initiate the growth of both particles and sheets (Fig. 7). Only the monomeric MgOH^+ cation (of several hypothetical $[\text{Mg}_p(\text{OH})_q]^{(2p-q)+}$ species) has been previously identified with confidence as forming prior to magnesium hydroxide (brucite) precipitation (typically at high pH) and at high temperature the cation's existence is fleeting at best.^{42,43} Al-

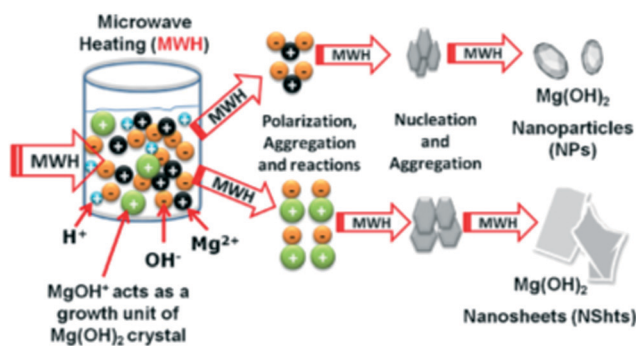


Fig. 7 Mechanism of crystal growth hypotheses by Al-Gaaneshi *et al.* reprinted from *Journal of Alloys and Compounds*, 521, R. Al-Gaashani, S. Radiman, Y. Al-Douri, N. Tabet and A. R. Daud, Investigation of the optical properties of $\text{Mg}(\text{OH})_2$ and MgO nanostructures obtained by microwave-assisted methods, 71–76, copyright 2012, with permission of Elsevier.⁴¹

Gaashani *et al.* also suggested (with reference to $\text{Zn}(\text{OH})_2/\text{ZnO}$ formation) that the exposure of the reactant solution to MW irradiation without stirring could promote differences in the temperature distribution and to the viscosity of the solution, leading ultimately to different morphologies.⁴⁴ In fact, if one considers this non-uniform temperature profile and the relative stability of the cations, it is perhaps not unreasonable to suppose that the formation of $[\text{MgOH}]^+$ is localised and crystallite formation could proceed either directly from Mg^{2+} or *via* the hydroxo cation.

In 2015, a surfactant-free hydrothermal MW synthesis inside a multimode cavity MW reactor was proposed, which could yield gram-quantities of single-phase nano- $\text{Mg}(\text{OH})_2$ from only MgO and without the use of additives.⁶ The synthesis was performed hydrothermally in a Teflon-lined autoclave and the reaction time could be decreased from 6 to 2 minutes by increasing the incident power from 750 to 800 W. The hexagonal nanoplates so-produced were 100–600 nm across and with a typical thickness of 10–60 nm (Fig. 8). The experimental hydrothermal procedure followed is broadly the microwave analogue to the conventional one proposed by Yu *et al.*¹¹ The mechanism of crystal growth proposed for the MW-HT synthesis contrasts slightly with the one suggested by Yu *et al.* and it consists of dissolution–precipitation steps followed by crystallite growth (eqn (3), Fig. 9).

The use of MWs results in a much higher rate of both heating and cooling and this could lead to an extremely fast initial MgO dissolution step (the solubility of MgO and $\text{Mg}(\text{OH})_2$ increases with increasing temperature^{45,46}). This is believed to be followed by the formation of magnesium hydroxide on the oxide surface *via* intermediate $\text{Mg}(\text{OH})^+$ species and then by the removal of $\text{Mg}(\text{OH})_2$ from the MgO surface (eqn (4)).^{47,48}

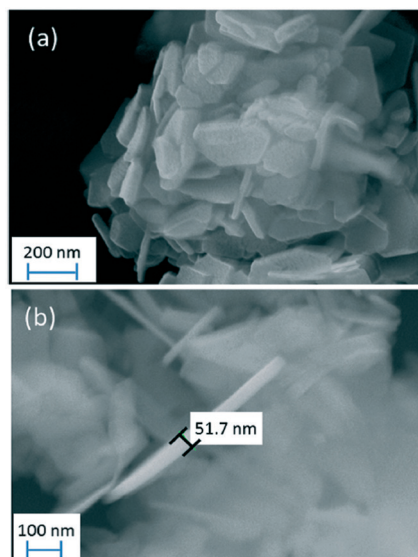


Fig. 8 (a) SEM micrograph of hexagonal nanoplates of $\text{Mg}(\text{OH})_2$ obtained in 4 minutes at 800 W; (b) SEM micrograph showing the thickness of individual nanoplates from the same sample. Reproduced from ref. 6 with permission from the Royal Society of Chemistry.



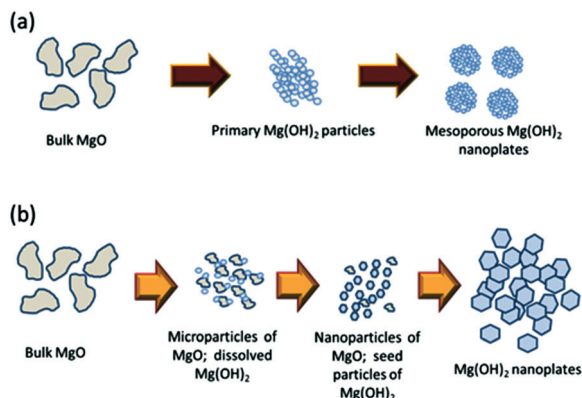
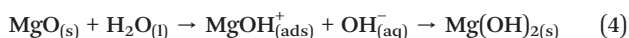


Fig. 9 Proposed growth processes for (a) conventional hydrothermal synthesis proposed by Yu *et al.*¹¹ and (b) MW-hydrothermal synthesis proposed by Hanlon *et al.*⁶ reproduced from ref. 6 with permission from the Royal Society of Chemistry.



The possible agglomeration of the particles is believed to occur on cooling. The mechanism (Fig. 9b) shows that the use of templating agents or surfactants is not essential for the synthesis of nano-MH, but that their use could help in suppressing the agglomeration of the nanoparticles, resulting in an increased surface area. Yu *et al.* had previously proposed that in conventional hydrothermal synthesis the agglomeration of small primary nanoparticles into nanoplates leads to the formation of a bimodal distribution of mesopores.¹¹

Precipitation methods

Solution based precipitation and co-precipitation methods are attractive ways to prepare MH under relatively mild conditions. Routes with and without the use of surfactants and surface modifiers have been explored as means to obtain nanostructures with controlled size and morphology

(Table 3). In 1993, Láska *et al.* started studying the influence of experimental parameters on the size distribution of magnesium hydroxide prepared by hydrating magnesium oxide, concluding that increasing the pH of the solutions resulted in a smaller crystal size, whereas raising the reaction temperature resulted in the opposite effect.⁴⁹ Ten years later, Henrist *et al.* conducted a systematic and wide-ranging investigation of the influence of a host of synthesis parameters including the chemical nature of magnesium precursors with different counter-ions (MgCl_2 and $\text{Mg}(\text{NO}_3)_2$), the chemical nature of the basic precipitating agent (NaOH , NH_4OH) and the variation in reaction temperature. The ambient pressure precipitation process was also compared to hydrothermal syntheses.⁵⁰ It was reported that the use of sodium hydroxide results in the preparation of “cauliflower-like” agglomerates, whilst the use of aqueous ammonia leads to the formation of hexagonal platelets. This contrast was attributed to the influences of pH and cation structure in solution. Also, as one might expect, the temperature has a strong effect, affecting the degree of agglomeration of the precipitated nanoparticles. Notably, particles tend to intergrow (agglomerate) at 60 °C and above, whereas at lower temperature, single, pseudo-circular platelets are obtained. A comparatively mild (180 °C; 14 h) hydrothermal treatment results in an increased mean particle size and decreased specific surface area.

In 2007, Zou *et al.* reported the synthesis of lamellar MH nanostructures obtained from the oxidation of magnesium metal in a mixture of formamide and water.⁵¹ The proposed one-step synthesis produces densely packed layers of agglomerated $\text{Mg}(\text{OH})_2$ particles as a result of simply immersing magnesium ribbons in a 6% formamide/water mixture at 80 °C for 12 h. Further, as shown in Fig. 10, the growth of the lamellar structures could be moderated as a function of reaction time when using a 4% formamide/water mixture at 80 °C. Initial Mg oxidation was very slow, limiting the Mg concentration and inducing heterogeneous nucleation preferentially on the metal substrate. As the reaction time increased, Mg species originating from the thermal decomposition of

Table 3 Effect of experimental parameters on MH products in selected examples of aqueous (co-)precipitation syntheses

Mg source	Additives	pH	T/K	Morphology	Dimensions	Ref.
MgO	NaOH/NH ₃ , TEA	10.2–13.0	393–413	Lamellar	Ave. diameter: 1.5–3.4 μm ^c	49
MgCl ₂ /Mg(NO ₃) ₂	NaOH/NH ₄ OH	ca. 10–13	283–313	“Cauliflower” agglomerates /lamellar ^a	Sphere diameter: ca. 300 nm; plate diameter ca. 200–450 nm ^f	50
Mg(NO ₃) ₂ ·6H ₂ O	NaOH, urea/EtOH	^b	333	Lamellar	Diameter: 50–200 nm ^f	52
MgSO ₄	NaOH, MgSA, CuSO ₄ ·5H ₂ O	^b	273–353	Lamellar/rod-like ^c	Plate diameter: ~50–100 nm; rod length: ~100–300 nm, rod diameter: ~10–30 nm ^f	54
MgCl ₂ ·6H ₂ O	NaOH, ODP	^b	^b	Lamellar	Diameter: ~100 nm; thickness: ~35 nm ^f	55
Mg(NO ₃) ₂ ·6H ₂ O	NaOH, SDS, MAP	^b	358	Lamellar	Diameter: ~100 nm ^f	56
MgCl ₂ ·6H ₂ O	NH ₄ OH, PEG 400	^b	323	Lamellar	Diameter: ~100 nm; thickness: 10–20 nm ^f	12
MgCl ₂ ·6H ₂ O	NH ₄ OH, PEG 12000	^b	293–353	Needle-like/lamellar	Needle length: ~1 μm; plate diameter: ~200 nm ^f	57
MgSO ₄	NaOH, PEG 200/PEG 8000/PEG 20000	^b	353	Lamellar	Diameter: ~30 nm–5 μm ^{d,f}	58
MgSO ₄	NaOH, OA, PMMA	^b	343	Lamellar	Diameter: ~100 nm ^f	60

^a Aggregates of spherical particles from NaOH, lamellae from NH₄OH. ^b Not reported. ^c Rods formed on addition of CuSO₄·5H₂O. ^d Dispersed best with PEG 200. ^e Agglomerated. ^f Dispersed.



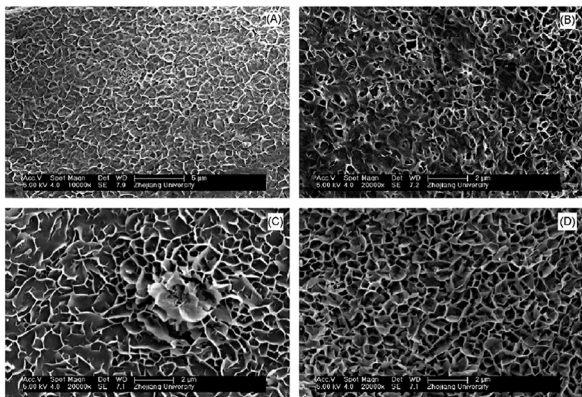


Fig. 10 Time-dependent evolution of magnesium hydroxide particle crystal morphology at different stages for Mg metal immersed in a 4% formamide/water solution at 80 °C: (A) 1 h, (B) 2 h, (C) 3 h, (D) 6 h, respectively. Reprinted from *Materials Research Bulletin*, 42, G. Zou, R. Liu, W. Chen, Z. Xu, Preparation and characterization of lamellar-like Mg(OH)₂ nanostructures *via* natural oxidation of Mg metal in formamide/water mixture, 1153–1158, copyright 2017, with permission of Elsevier.⁵¹

Mg–formamide complexes were continuously supplied for subsequent crystal growth on heterogeneous nuclei. Fig. 10(a) shows that at 1 h rod-like nuclei grow on the substrate from heterogeneous nucleation of MH. At 2 h, the nuclei start to branch on the surface, gradually forming the beginnings of a 3D porous skeleton for further growth (Fig. 10(b)). By 6 h into the nucleation and growth process, the lamellar MH structures develop into a continuous porous network (Fig. 10(d)).

An alternative surfactant-free precipitation route to lamellar MH nanoparticles is possible *via* reaction of aqueous solutions of magnesium chloride hexahydrate and sodium hydroxide in the presence/absence of urea and/or ethanol.⁵² Addition of ethanol apparently produced more regular hexagonal lamellae. Although no surfactants were employed, urea evidently prevented agglomeration presumably by coordinating to Mg²⁺ in solution. Moreover, chloride impurities were reduced on urea addition. In fact, an earlier study showed similar nanostructured MH lamellae could be obtained from lower concentrations of the same reactants without the use of urea (or other structure directing additives).¹⁵

Although surfactant-free syntheses are environmentally favourable, there is no doubt that a very high level of control over size and morphology of nanomaterials can be achieved when employing surfactants, dispersants and surface modifiers in precipitation processes. Over a decade ago, Lv *et al.* were able to produce MH nanoparticles with three different morphologies exploiting the precipitation process of a magnesium precursor species (MgCl₂·6H₂O) in the presence of different complex dispersants and surfactants.⁵³ In their comprehensive study, they also studied the influence of synthesis parameters such as temperature, concentration and type of precipitating reagent (NH₄OH, NaOH). A multitude of additives were investigated; gelatin, lauryl sodium sulfate,

polyvinylpyrrolidone, polyglycol ether, polysorbate 80, polyvinyl alcohol, sodium polymethacrylate and polyacrylamide. By tuning the various reaction conditions, it was possible to obtain needle-, lamellar- and rod-like nanoparticles selectively. Although the selection of complex dispersant/surfactant was instrumental in checking growth and controlling size distribution, the alkali solution concentration appeared to be more important in controlling morphology. The use of lower concentration aqueous ammonia (5 wt%) promoted the formation of 1D structures, whereas a higher concentration (25 wt%) promoted the formation of lamellae. It was proposed that the polymer dispersants exert more structural control at the lower NH₃(aq) concentration, anisotropically limiting the growth of crystal nuclei resulting in needle-like particles which became rods when ammonia was added at a much slower rate. At the higher NH₃(aq) concentration, the structure directing effect of the dispersants was less significant and crystal nuclei agglomerate and form lamellar-like particles.

Morphological selectivity was also achieved in the presence of magnesium stearate (MgSA) as a surfactant, although as in the example above, the two different observed morphologies of MH (lamellar and rod-like particles) were more likely determined by other factors.⁵⁴ Magnesium(II) sulfate and NaOH solution were used to coprecipitate MH in the presence of MgSA. Notably, it was only possible to move from growth of MH lamellae to rod-like MH crystals when copper(II) salts were added. The premise was presented that similarly sized Cu²⁺ could partly replace Mg²⁺ within individual octahedra in the MH structure during crystallization. It was proposed that adding Cu²⁺ (0.4 mol%) into magnesium salt solution moderates growth in specific directions to form rod-like nuclei, which evolve into rod-like crystals. NaOH concentration, reaction time and temperature were also deemed significant (by increasing the temperature from close to 0 °C through 50 °C to 80 °C, the morphology switched from lamellae to rods back to lamellae) mediating the kinetics of Cu²⁺ diffusion. Ultimately, the role of Cu(II) salts in the growth mechanism is unresolved and whether Cu²⁺ is included in the MH crystal structure, for example, is unclear.

Octadecyl dihydrogen phosphate (ODP) was proposed to check crystal growth by surface modification.⁵⁵ In a simple one-step wet precipitation process, Mg(OH)₂ nanoparticles were prepared from magnesium chloride hexahydrate, sodium hydroxide and ODP. ODP was proposed to engender hydrophobic (001) surfaces and thus restrict the crystal growth in the *c* direction. Lamellar nano-Mg(OH)₂ plates synthesised in the presence of ODP grew with an average lateral dimension of 60 nm and an average thickness of *ca.* 35 nm whereas an average lateral dimension of 130 nm and an average thickness of *ca.* 20 nm predominated when no surface modifier was employed. Similarly sodium dodecyl sulfate (SDS) and monoalcohol ether phosphate (MAP) (2 : 1 by weight) were applied as surface-modifiers in an MH co-precipitation starting from magnesium nitrate hexahydrate and NaOH.⁵⁶ Addition of SDS/MAP in different amounts from 0.0 to 1.0 wt% had



- 20 A. N. Christensen, P. Norby and J. C. Hanson, *J. Solid State Chem.*, 1995, **114**, 556–559.
- 21 W. Fan, S. Sun, X. Song, W. Zhang, H. Yu, X. Tan and G. Cao, *J. Solid State Chem.*, 2004, **177**, 2329–2338.
- 22 P. Jeevanandam, R. S. Mulukutla, Z. Yang, H. Kwen and K. J. Klabunde, *Chem. Mater.*, 2007, **19**, 5395–5403.
- 23 L. Zhuo, J. Ge, L. Cao and B. Tang, *Cryst. Growth Des.*, 2009, **9**, 1–6.
- 24 Y. Chen, T. Zhou, H. Fang, S. Li, Y. Yao and Y. He, *Procedia Eng.*, 2015, **102**, 388–394.
- 25 H. Yan, X. Zhang, J. Wu, L. Wei, X. Liu and B. Xu, *Powder Technol.*, 2008, **188**, 128–132.
- 26 Q. L. Wu, L. Xiang and Y. Jin, *Powder Technol.*, 2006, **165**, 100–104.
- 27 H. Dhaouadi, H. Chaabane and F. Touati, *Nano-Micro Lett.*, 2011, **3**, 153–159.
- 28 X. T. Sun, L. Xiang, C. Zhu and Q. Liu, *Cryst. Res. Technol.*, 2008, **43**, 1057–1061.
- 29 B. Jia and L. Gao, *J. Am. Ceram. Soc.*, 2006, **89**, 3881–3884.
- 30 S. Elbasuney and S. F. Mostafa, *Powder Technol.*, 2015, **278**, 72–83.
- 31 D. Jin, X. Gu, X. Yu, G. Ding, H. Zhu and K. Yao, *Mater. Chem. Phys.*, 2008, **112**, 962–965.
- 32 Q. Wang, C. Li, M. Guo, L. Sun and C. Hu, *Mater. Res. Bull.*, 2014, **51**, 35–39.
- 33 H. J. Kitchen, S. K. Vallance, J. L. Kennedy, N. Tapia-Ruiz, L. Carassiti, A. Harrison, A. G. Whittaker, T. D. Drysdale, S. W. Kingman and D. H. Gregory, *Chem. Rev.*, 2014, **114**, 1170–1206.
- 34 I. Bilecka and M. Niederberger, *Nanoscale*, 2010, **2**, 1358.
- 35 Y.-J. Zhu and F. Chen, *Chem. Rev.*, 2014, **114**, 6462–6555.
- 36 K. L. Harrison and A. Manthiram, *Chem. Mater.*, 2013, **25**, 1751–1760.
- 37 J. Zhao and W. Yan, in *Modern Inorganic Synthetic Chemistry*, ed. R. Xu, W. Pang and Q. Huo, Elsevier, Amsterdam, Editon edn, 2011, pp. 173–195.
- 38 H. Wu, M. Shao, J. Gu and X. Wei, *Mater. Lett.*, 2004, **58**, 2166–2169.
- 39 K. M. Saoud, S. Saeed, R. M. Al-Soubaihi and M. F. Bertino, *Am. J. Nanomater.*, 2014, **2**, 21–25.
- 40 Y. Hattori, S. Mukasa, H. Toyota, T. Inoue and S. Nomura, *Mater. Chem. Phys.*, 2011, **131**, 425–430.
- 41 R. Al-Gaashani, S. Radiman, Y. Al-Douri, N. Tabet and A. R. Daud, *J. Alloys Compd.*, 2012, **521**, 71–76.
- 42 P. L. Brown, S. E. Drummond Jr. and D. A. Palmer, *J. Chem. Soc., Dalton Trans.*, 1996, 3071–3075.
- 43 D. A. Palmer and D. J. Wesolowski, *J. Solution Chem.*, 1997, **26**, 217–232.
- 44 R. Al-Gaashani, S. Radiman, N. Tabet and A. R. Daud, *Mater. Chem. Phys.*, 2011, **125**, 846–852.
- 45 H. Remy and A. Kuhlmann, *Z. Anal. Chem.*, 1924, **65**, 1.
- 46 J. K. Gjaldbaek, *Z. Anorg. Allg. Chem.*, 1925, **144**, 145.
- 47 G. L. Smithson and N. N. Bakhshi, *Can. J. Chem.*, 1969, **47**, 508–513.
- 48 S. D. Rocha, M. B. Mansur and V. S. Ciminelli, *J. Chem. Technol. Biotechnol.*, 2004, **79**, 816–821.
- 49 M. Láska, J. Valtýni and P. Fellner, *Cryst. Res. Technol.*, 1993, **28**, 931–936.
- 50 C. Henrist, J. P. Mathieu, C. Vogels, A. Rulmont and R. Cloots, *J. Cryst. Growth*, 2003, **249**, 321–330.
- 51 G. Zou, R. Liu, W. Chen and Z. Xu, *Mater. Res. Bull.*, 2007, **42**, 1153–1158.
- 52 W. Jiang, X. Hua, Q. Han, X. Yang, L. Lu and X. Wang, *Powder Technol.*, 2009, **191**, 227–230.
- 53 J. Lv, L. Qiu and B. Qu, *J. Cryst. Growth*, 2004, **267**, 676–684.
- 54 D. Chen, L. Zhu, H. Zhang, K. Xu and M. Chen, *Mater. Chem. Phys.*, 2008, **109**, 224–229.
- 55 D. An, L. Wang, Y. Zheng, S. Guan, X. Gao, Y. Tian, H. Zhang, Z. Wang and Y. Liu, *Colloids Surf., A*, 2009, **348**, 9–13.
- 56 H. Dong, Z. Du, Y. Zhao and D. Zhou, *Powder Technol.*, 2010, **198**, 325–329.
- 57 P. Wang, C. Li, H. Gong, H. Wang and J. Liu, *Ceram. Int.*, 2011, **37**, 3365–3370.
- 58 A. Pilarska, M. Wysokowski, E. Markiewicz and T. Jesionowski, *Powder Technol.*, 2013, **235**, 148–157.
- 59 J. Zheng and W. Zhou, *Mater. Lett.*, 2014, **127**, 17–19.
- 60 H. Yan, X. Zhang, L. Wei, X. Liu and B. Xu, *Powder Technol.*, 2009, **193**, 125–129.
- 61 E. J. McHenry, *Electrochem. Technol.*, 1967, **5**, 275.
- 62 G. H. A. Therese and P. V. Kamath, *J. Appl. Electrochem.*, 1998, **28**, 539–543.
- 63 M. Dinamani and P. V. Kamath, *J. Appl. Electrochem.*, 2004, **34**, 899–902.
- 64 G. Zou, R. Liu and W. Chen, *Mater. Lett.*, 2007, **61**, 1990–1993.
- 65 G. Zou, W. Chen, R. Liu and Z. Xu, *Mater. Chem. Phys.*, 2008, **107**, 85–90.
- 66 L. Hao, C. Zhu, X. Mo, W. Jiang, Y. Hu, Y. Zhu and Z. Chen, *Inorg. Chem. Commun.*, 2003, **6**, 229–232.
- 67 C. Liang, T. Sasaki, Y. Shimizu and N. Koshizaki, *Chem. Phys. Lett.*, 2004, **389**, 58–63.
- 68 X. Li, C. Ma, J. Zhao, Z. Li, S. Xu and Y. Liu, *Powder Technol.*, 2010, **198**, 292–297.
- 69 A. Pilarska, L. Klapiszewski and T. Jesionowski, *Powder Technol.*, 2017, **319**, 373–407.
- 70 L. Qiu, R. Xie, P. Ding and B. Qu, *Compos. Struct.*, 2003, **62**, 391–395.
- 71 J. Lv and W. Liu, *J. Appl. Polym. Sci.*, 2007, **105**, 333–340.
- 72 H. Gui, X. Zhang, Y. Liu, W. Dong, Q. Wang, J. Gao, Z. Song, J. Lai and J. Qiao, *Compos. Sci. Technol.*, 2007, **67**, 974–980.
- 73 R. Suihkonen, K. Nevalainen, O. Orell, M. Honkanen, L. Tang, H. Zhang, Z. Zhang and J. Vuorinen, *J. Mater. Sci.*, 2011, **47**, 1480–1488.
- 74 H. Li, S. Liu, J. Zhao and N. Feng, *Colloids Surf., A*, 2016, **494**, 222–227.
- 75 K. Wang, J. Zhao, H. Li, X. Zhang and H. Shi, *J. Taiwan Inst. Chem. Eng.*, 2016, **61**, 287–291.
- 76 M. El Bouraie and A. A. Masoud, *Appl. Clay Sci.*, 2017, **140**, 157–164.
- 77 N. A. Oladoja, S. Chen, J. E. Drewes and B. Helmreich, *Chem. Eng. J.*, 2015, **281**, 632–643.



- 78 A. Umar, F. Al-Hazmi, G. N. Dar, S. A. Zaidi, R. M. Al-Tuwirqi, F. Alnowaiserb, A. A. Al-Ghamdi and S. W. Hwang, *Sens. Actuators, B*, 2012, **166–167**, 97–102.
- 79 M. M. Rahman, A. Jamal, S. B. Khan and M. Faisal, *J. Phys. Chem. C*, 2011, **115**, 9503–9510.
- 80 C. Dong, J. Cairney, Q. Sun, O. L. Maddan, G. He and Y. Deng, *J. Nanopart. Res.*, 2010, **12**, 2101–2109.
- 81 C. Dong, G. He, W. Zheng, T. Bian, M. Li and D. Zhang, *Mater. Lett.*, 2014, **134**, 286–289.
- 82 J. Liu, W. Wang, Z. Guo, R. Zeng, S. Dou and X. Chen, *Chem. Commun.*, 2010, **46**, 3887.
- 83 A. Kumar and J. Kumar, *J. Phys. Chem. Solids*, 2008, **69**, 2764–2772.
- 84 N. C. S. Selvam, R. T. Kumar, L. J. Kennedy and J. J. Vijaya, *J. Alloys Compd.*, 2011, **509**, 9809–9815.
- 85 L. Kumari, W. Z. Li, C. H. Vannoy, R. M. Leblanc and D. Z. Wang, *Ceram. Int.*, 2009, **35**, 3355–3364.
- 86 N. M. Julkapli and S. Bagheri, *Rev. Inorg. Chem.*, 2015, **36**, 1–41.
- 87 B. Nagappa and G. T. Chandrappa, *Microporous Mesoporous Mater.*, 2007, **106**, 212–218.
- 88 F. Luo, J. Lu, W. Wang, F. Tan and X. Qiao, *Micro Nano Lett.*, 2013, **8**, 479.
- 89 G. Sung, J. W. Kim and J. H. Kim, *J. Ind. Eng. Chem.*, 2016, **44**, 99–104.
- 90 F. K. V. Moreira, D. C. A. Pedro, G. M. Glenn, J. M. Marconcini and L. H. C. Mattoso, *Carbohydr. Polym.*, 2013, **92**, 1743–1751.
- 91 C. H. Kum, Y. Cho, Y. K. Joung, J. Choi, K. Park, S. H. Seo, Y. S. Park, D. J. Ahn and D. K. Han, *J. Mater. Chem. B*, 2013, **1**, 2764.
- 92 C. Dong, G. He, H. Li, R. Zhao, Y. Han and Y. Deng, *J. Membr. Sci.*, 2012, **387–388**, 40–47.
- 93 S. Jahangiri and N. J. Mosey, *Phys. Chem. Chem. Phys.*, 2017, **19**, 1963.

